Biochemistry

 Volume 36, Number 4 January 28, 1997

Accelerated Publications

Structure of Bacterial Luciferase β_2 Homodimer: Implications for Flavin Binding[†,‡]

John J. Tanner,[§] Mitchell D. Miller,[§] Keith S. Wilson,[||] Shiao-Chun Tu,[§] and Kurt L. Krause*[,§]

Department of Biochemical and Biophysical Sciences, University of Houston, Houston, Texas 77204-5934, and European Molecular Biology Laboratory, Hamburg Outstation, c/o DESY, Notkestrasse 85, 2000 Hamburg, Germany

Received October 7, 1996; Revised Manuscript Received November 25, 1996[⊗]

ABSTRACT: The crystal structure of the β_2 homodimer of *Vibrio harveyi* luciferase has been determined to 2.5 Å resolution by molecular replacement. Crystals were grown serendipitously using the $\alpha\beta$ form of the enzyme. The subunits of the homodimer share considerable structural homology to the β subunit of the $\alpha\beta$ luciferase heterodimer. The four C-terminal residues that are disordered in the $\alpha\beta$ structure are fully resolved in our structure. Four peptide bonds have been flipped relative to their orientations in the β subunit of the $\alpha\beta$ structure. The dimer interface of the homodimer is smaller than the interface of the heterodimer in terms of buried surface area and number of hydrogen bonds and salt links. Inspection of the subunits of our structure suggests that $FMNH_2$ cannot bind to the β_2 enzyme at the site that has been proposed for the $\alpha\beta$ enzyme. However, we do uncover a potential $FMNH_2$ binding pocket in the dimer interface, and we model FMN into this site. This proposed flavin binding motif is consistent with several lines of biochemical and structural evidence and leads to several conclusions. First, only one $FMNH_2$ binds per homodimer. Second, we predict that reduced FAD and riboflavin should be poor substrates for β_2. Third, the reduced activity of β_2 compared to $\alpha\beta$ is due to solvent exposure of the isoalloxazine ring in the β_2 active site. Finally, we raise the question of whether our proposed flavin binding site could also be the binding site for flavin in the $\alpha\beta$ enzyme.

Luciferases are enzymes that catalyze the production of light, and they are of interest for both basic and practical reasons (Baldwin & Ziegler, 1992; Tu & Mager, 1995). In vivo, they are responsible for the glow observed in luminous bacteria, fireflies, and other organisms. There is the biological question of why these organisms emit light. From the chemical point of view, there is intense interest in learning how bacterial luciferase can generate light from aldehyde, molecular oxygen, and $FMNH_2$ (eq 1). In vitro, luciferase is used in a variety of biotechnological applications such as monitoring gene expression. In this area there are efforts to modify and enhance the activity of luciferase, for example,

$$FMNH_2 + RCHO + O_2 \xrightarrow{\text{bacterial luciferase}} FMN + RCOOH + H_2O + \text{light} \quad (1)$$

to alter its emission spectrum, substrate specificity, and thermal stability.

The most active form of bacterial luciferase is an $\alpha\beta$ heterodimer, whose crystal structure was recently determined under high salt conditions at 2.4 Å resolution (Baldwin et al., 1995; Fisher et al., 1995) and in low salt conditions at 1.5 Å resolution (Fisher et al., 1996). Bacterial luciferase also forms an active β_2 homodimer, which is the subject of this report. The β_2 homodimer is 5 orders of magnitude less active than the $\alpha\beta$ enzyme; however, the reason for its decreased activity is not fully understood (Choi et al., 1995; Sinclair et al., 1993). The fact that β_2 is active at all is intriguing since the crystal structure of the $\alpha\beta$ enzyme suggests that the $FMNH_2$ binding site resides entirely in the α subunit and that many of the putative active site residues are not conserved in the β subunit. Identification of the active site of β_2 would help to explain how β_2 can actually

[†] This work was supported by the National Institutes of Health (GM25953, S.-C.T.), the Robert A. Welch Foundation (E-1030, S.-C.T.), the State of Texas (K.L.K. & S.-C.T.), and the W. M. Keck Foundation.

[‡] Coordinates have been deposited in the Brookhaven Protein Data Bank under ID code 1xkj.

* Corresponding author. Email: kkrause@uh.edu.

[§] University of Houston.

[||] European Molecular Biology Laboratory.

[⊗] Abstract published in *Advance ACS Abstracts*, January 1, 1997.

S0006-2960(96)02511-1 CCC: $14.00

catalyze the bioluminescence reaction and why the heterodimer is so much more active.

The discovery that bacterial luciferase can form a homodimer was made almost 30 years ago. The record, however, is confusing due to a change in the nomenclature for the subunits. The ability of the isolated β subunit from the *Photobacterium fischeri* luciferase to form a β_2 homodimer was first described in 1967 (Friedland & Hastings, 1967). For the *Vibrio harveyi* (originally designated as strain MAV) luciferase, the formation of the α_2 dimer was also reported in 1969 (Hastings et al., 1969). The original designations of the α and β subunits in these two reports were both based on charge properties but were later redefined to assign α and β to the heavy (40 kDa) and light (35 kDa) subunits, respectively, of the heterodimer (Gunsalus-Miguel et al., 1972; Ruby & Hastings, 1980). This now widely accepted classification does not change the designation of the *P. fischeri* luciferase subunits but reverses that for the α and β subunits of the *V. harveyi* luciferase (Gunsalus-Miguel et al., 1972). Therefore, the homodimers derived from the *P. fischeri* and *V. harveyi* luciferase subunits (Hastings et al., 1969) are both β_2. In the present paper, we use the now widely accepted nomenclature based on molecular weight and use the terms α and β for the 40 kDa and 35 kDa subunits of *V. harveyi* luciferase, respectively. We refer to the two β subunits of our homodimer structure as subunit A and subunit B.

The binding and dissociation rate constants for the *V. harveyi* β dimerization reaction recently have been quantified (Sinclair et al., 1994). Moreover, the low but genuine bioluminescence activity reported for the individual β subunit from *V. harveyi* luciferase (Sinclair et al., 1993; Waddle & Baldwin, 1991) has been shown to be associated with β_2 (Choi et al., 1995) and not due to isolated β subunits.

Interestingly, if one uses up to 1 μM $FMNH_2$ and 1 μM decanal for the luminescence reaction, β_2 is found to contain a single binding site for each of these two substrates. At higher concentrations of decanal, the binding of a second aldehyde by β_2 at an inhibitor site is also detected. This inhibition is attributed to blockage of the $FMNH_2$ binding site (Choi et al., 1995). The location of these substrate and inhibitor sites in β_2 remains an intriguing question.

The structure of β_2 is being studied by another group (Baldwin et al., 1995, 1997), but to our knowledge a full report of their findings has not been published, nor is their structure available from the protein data bank. Therefore, we are unable to make any direct comparisons with our structure.

MATERIALS AND METHODS

Crystallization and X-ray Data Collection. A recombinant plasmid, pTH3, was constructed by subcloning the *lux*AB-containing *Sal*I−*Bgl*II fragment (with the *Bgl*II end blunted for ligation) of pTH2 (Xi et al., 1990) into pUC19 at the *Sal*I and *Sma*I sites. The *lux*AB genes encoding the *V. harveyi* heterodimeric luciferase were expressed (Xi et al., 1990) in *Escherichia coli* JM101 harboring pTH3. Luciferase was purified as described previously (Cousineau & Meighen, 1976) and involves (aminohexyl)agarose column chromatography for the last step of purification.

Purified $\alpha\beta$ luciferase was dialyzed prior to crystallization versus 10 mM piperazine-*N*,*N*′-bis(2-ethanesulfonic acid) (PIPES)[1] plus 10 mM DL-dithiothreitol (DTT) at pH 6.8, concentrated to 50 mg/mL, and filtered through a 0.22 μm filter. Crystals were grown at 4 °C in sitting drops using a reservoir solution of 12% poly(ethylene glycol) 4000, 17−21% 2-propanol, 6 mM DTT, and 0.1 M citrate, pH 6.2. A heavy precipitate forms initially, and after 4−8 weeks octahedral crystals of size 0.4 × 0.4 × 0.6 mm are found buried under the precipitate.

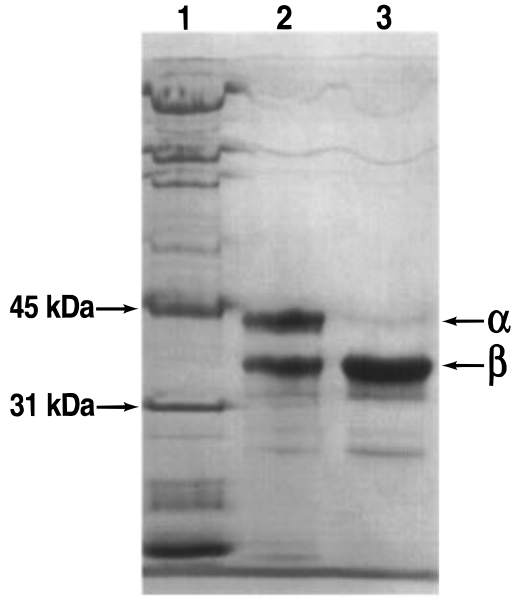

FIGURE 1: 12.5% homogeneous SDS−PAGE gel run on a Pharmacia Phast system and stained with Coomassie blue R-350. Lanes: 1, Bio-Rad broad range molecular weight markers; 2, enzyme before crystallization; 3, dissolved crystals.

We were surprised to discover that we had crystallized the β_2 form of the enzyme. In fact, this realization was not made until the initial stages of structure refinement. SDS gel electrophoresis (Figure 1), performed after the structure was solved, confirmed that the crystals are composed of only β subunits even though the protein used to grow the crystals contained both α and β subunits.

It appears that at some point during our procedure the $\alpha\beta$ dimer interface was disrupted and the heterodimer decomposed into α and β subunits, followed by dimerization of the β subunits. Since the freshly purified enzyme displayed activity levels characteristic of the $\alpha\beta$ form, conversion to the β_2 form must have occurred either in the PIPES dialysis step or in the actual crystallization step.

Crystals were stabilized for data collection at room temperature in 16% PEG, 16% 2-propanol, 2 mM DTT, and 0.1 M citrate, pH 6.0. The space group was determined using precession photographs obtained with an Enraf-Nonius precession camera with a crystal to film distance of 100 mm mounted on an FR590 sealed tube X-ray source operated at 40 kV and 45 mA. Photographs of the three principal zones revealed 4/*mmm* reciprocal space symmetry and systematic absences consistent with the enantiomorphous space groups $P4_12_12$ and $P4_32_12$. The correct choice of space group, as found from translation function calculations, is $P4_12_12$.

Native data to 2.5 Å were collected at room temperature on DESY/EMBL beamline BW7B with a wavelength of 0.865 Å using an 18 cm MAR image plate detector. The

[1] Abbreviations: PIPES, piperazine-*N*,*N*′-bis(2-ethanesulfonic acid); DTT, DL-dithiothreitol; RMSD, root mean square difference; A_s, solvent-accessible surface area.

crystal to film distance was 250 mm and the detector θ angle was 0. The frame width was 1° and the exposure time was approximately 40 s. Data were processed with Denzo and Scalepack (Minor, 1993; Otwinowski, 1993). The refined unit cell dimensions are $a = b = 112.4$ Å and $c = 153.7$ Å with one homodimer per asymmetric unit. The final data set consists of 97 frames of data merged from two crystals and contains 245 416 observations of 32 225 unique reflections with a merging *R*-factor (on intensities) of 8.8%. These data are 93% complete to 2.5 Å and 78% complete in the 2.6−2.5 Å bin.

Molecular Replacement and Refinement. Initial phases were determined by molecular replacement. All molecular replacement and structure refinement calculations were carried out in X-PLOR version 3.1 (Brünger, 1992). The Engh and Huber force field (Engh & Huber, 1991) was used during simulated annealing and conjugate gradient minimization but was modified by eliminating hydrogen atoms and disabling the nonbonded electrostatics terms. A σ cutoff for reflections was not used during molecular replacement and refinement. Individual *B*-factors were refined using restraints to standard deviations of 1.0 Å^2 for main chain bonded atoms, 1.5 Å^2 for side chain bonded atoms, 1.5 Å^2 for main chain atoms related by bond angles, and 2.0 Å^2 for side chain atoms related by bond angles. Noncrystallographic symmetry restraints were not used during refinement. O (Jones et al., 1991) was used for model building.

The search model for molecular replacement was the 2.4 Å *V. harveyi* luciferase $\alpha\beta$ heterodimer (Fisher et al., 1995; pdb code 1brl) because at the time we thought we had crystallized the $\alpha\beta$ enzyme. Since the α and β subunits share high sequence and structural homology, an $\alpha\beta$ search model was appropriate. The sequences are 32% identical with the major difference being a 29-residue insert in α subunit. In the $\alpha\beta$ structure both subunits fold into eight-stranded β/α barrels and the core β-strands superimpose with a root mean square difference (RMSD) of 0.6 Å (Fisher et al., 1995, 1996).

Rotation function and Patterson correlation calculations at 10−4 Å resolution revealed two orientations with nearly identical scores. The search model was oriented according to the Patterson correlation peaks and input to translation function calculations (10−4 Å) followed by rigid body refinement (10−4 Å). Searches in space group $P4_32_12$ yielded incorrect solutions with *R*-factor > 50% after rigid body refinement. In space group $P4_12_12$, however, the two orientations from Patterson correlation refinement led to two translation function solutions with *R*-factor = 46% (10−4 Å) after rigid body refinement. In both cases, simulated annealing lowered the *R*-factor to 34% with $R_{free} = 44\%$ (15−2.5 Å). The fact that these two solutions were related to each other by the molecular 2-fold axis and had nearly identical *R*-factors was the first clue that we had crystallized the β_2 dimer. Indeed, in each solution the quality of the electron density was much better in the β subunit than in the α subunit. Another clue that we did not have $\alpha\beta$ crystals is the fact that R_{free} > 40% often is symptomatic of an incorrect structure (Kleywegt & Brünger, 1996). We note that the test set for R_{free} calculations was 10% of the entire data set and that the same test set was used for all refinement calculations.

We next constructed a β_2 homodimer from the two $\alpha\beta$ solutions found in space group $P4_12_12$. Rigid body refinement lowered the *R*-factor to 33% (10−4 Å), and simulated annealing resulted in *R*-factor = 26% and $R_{free} = 34\%$ (15−2.5 Å). The significant decrease in R_{free} indicated that replacement of the heterodimer by a homodimer was a correct move. Now the electron density was of high quality in both subunits. Also, electron density for the four C-terminal residues missing from the β subunit of the published $\alpha\beta$ structures could be seen in both subunits.

Several rounds of rebuilding and refinement were performed. Solvent was modeled in the final stages of refinement with a bulk solvent mask and discrete water molecules. Solvent sites were filled if they had at least a 3σ peak in the $F_o - F_c$ map and were covered by the $2F_o - F_c$ map contoured at 0.75σ. Water was inspected after refinement and those with either $B > 55$ Å^2 or that had weak or nonspherical $2F_o - F_c$ density were discarded.

In the next section, comparisons between the β_2 and $\alpha\beta$ structures were done using the 2.4 Å $\alpha\beta$ structure. The 1.5 Å $\alpha\beta$ structure was not available when our manuscript was submitted. We note that there are no significant differences between the two $\alpha\beta$ structures and that they superimpose with RMSD of 0.59 Å (Fisher et al., 1996).

RESULTS AND DISCUSSION

Quality of the Structure. The current model consists of 5092 atoms, including 648 amino acid residues and 31 water molecules. Fifteen surface side chains were omitted due to weak density. The *R*-factor is 19.1% for 28 976 reflections between 15 and 2.5 Å resolution with $R_{free} = 24.9\%$ (3249 reflections). The *R*-factor calculated against the entire data set is 19.7%.

A Luzzati plot (Luzzati, 1952) calculated using the working set of reflections suggests a mean positional error of about 0.25−0.35 Å. The error estimate from the Luzzati plot calculated with test reflections is about 0.35−0.40 Å. The RMS coordinate error estimates from σ_A (Read, 1986) are 0.32 Å for the working set and 0.37 Å for the test set. The geometry is tight, with RMS deviation from the ideal force field values of 0.013 Å for bonds, 1.6° for angles, 23.3° for dihedral angles, and 1.4° for improper dihedral angles. The stereochemistry meets or exceeds all main chain and side chain tests of PROCHECK version 3.4.2 (Laskowski et al., 1993). Over 99% of the non-Gly and non-Pro residues fall into the most favored or additionally allowed regions of the Ramachandaran plot. The four outliers (Asp A259, Asn B12, Ser B256, Asp B259) are in surface loops where the electron density is relatively weak.

The real space correlation (Jones et al., 1991) between the all-atom model and the final $2F_o - F_c$ map is in Figure 2. The average correlation coefficient is 0.92 and the standard deviation is 0.04. This plot indicates that the model fits the electron density well except in a few regions. For example, the electron density for the guanidinium group of Arg B15 is weak. Since the density for the main chain and most of the side chain is strong, we included the entire side chain in the model. It is built like Arg A15, which has stronger density and a higher correlation coefficient. The 250's loop in the B subunit is probably the least accurate part of the structure, and it has been built like the 250's loop in the β subunit of the 2.4 Å $\alpha\beta$ structure. In the A subunit the density is stronger and suggested a main chain conformation that is slightly different from that observed in the 2.4 Å $\alpha\beta$ structure.

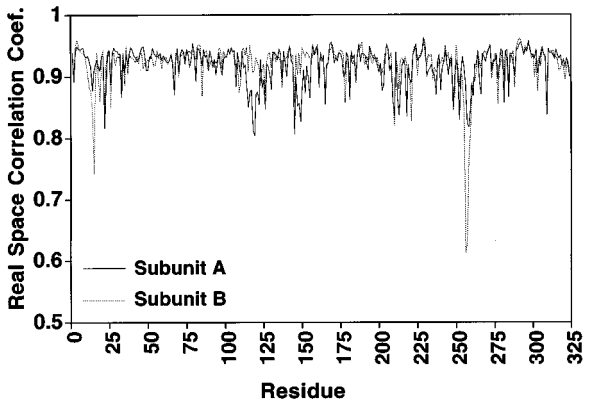

FIGURE 2: Real space correlation coefficients. The correlation is between the all-atom model and the final $2F_o - F_c$ map calculated with O rsr parameters $A_o = C = 0.9$.

The *B*-factors approximately track the real space correlation coefficients. The average *B*-factor for all atoms is 37.8 Å^2, while the average *B*-factor for solvent is 32.2 Å^2. The average *B*-factors for the A and B subunits are 40.9 and 34.9 Å^2, respectively. For comparison, the average *B*-factor of the β subunit of the 2.4 Å $\alpha\beta$ structure is 43 Å^2 (Fisher et al., 1995), while that of the 1.5 Å $\alpha\beta$ structure is 17 Å^2 (Fisher et al., 1996). The pattern of maxima and minima in our *B*-factors is similar to those of the $\alpha\beta$ structures.

Subunit Structure. The secondary and tertiary structures of the subunits of β_2 are very similar to those of the β subunit of $\alpha\beta$ luciferase. As expected, each subunit folds into the eight-stranded β/α barrel motif described previously for $\alpha\beta$ luciferase (Figure 3). The RMSD between the main chains of the two subunits of β_2 is 0.45 Å.

The main chain of our structure is similar to that of the β subunit of the $\alpha\beta$ structure (Figure 4). Note that the superimposition for the β-strands is almost perfect. The RMSD between the main chain of the β subunit of $\alpha\beta$ luciferase and the subunits of β_2 is 0.59 Å for subunit A of β_2 and 0.63 Å for subunit B of β_2. The secondary structure assignments are the same as those for the β subunit of the $\alpha\beta$ structure (Fisher et al., 1995).

The four C-terminal residues (321−324) that are missing from the β subunits of both $\alpha\beta$ structures are resolved in both subunits of our structure. These residues (Lys 321, Tyr 322, His 323, Ser 324) extend the C-terminal helix for another complete turn. Stabilization of the C-termini is due to crystal contacts (Figure 5). In both subunits the carboxylate group of Ser 324 of one subunit salt links with crystallographic mates of Arg 223 and the amino group of Met 1 of the other subunit. Likewise, His 323 of one subunit hydrogen bonds to a crystallographic mate of Tyr 322 of the other subunit. Thus, crystallographic symmetry brings the C-terminus of one subunit into contact with both the N- and C-termini of the other subunit.

Another deviation between the β_2 structure and the structure of the β subunit of $\alpha\beta$ concerns four peptide bonds. Our electron density unambiguously indicated that the peptide bonds between residues 146 and 147 and between residues 161 and 162 in both subunits should be flipped from their orientations in the β subunit of the 2.4 Å $\alpha\beta$ structure. Finally, there are 36 surface side chains (18 per subunit) whose torsion angles deviate significantly from the $\alpha\beta$ structure. We note that all of these side chains have atoms with *B*-factor = 100 Å^2 in the 2.4 Å $\alpha\beta$ structure, so it is not surprising that they display different conformations in the β_2 structure.

Since a comparison between the α and β subunits has been described previously (Baldwin et al., 1995; Fisher et al., 1995), we will note only a few points that impact our discussion of the active site. First, after the $\alpha\beta$ structure is superimposed on the β_2 structure, the inorganic PO_4 or SO_4 ion bound to the α subunit lands on the CA of Thr 175 of

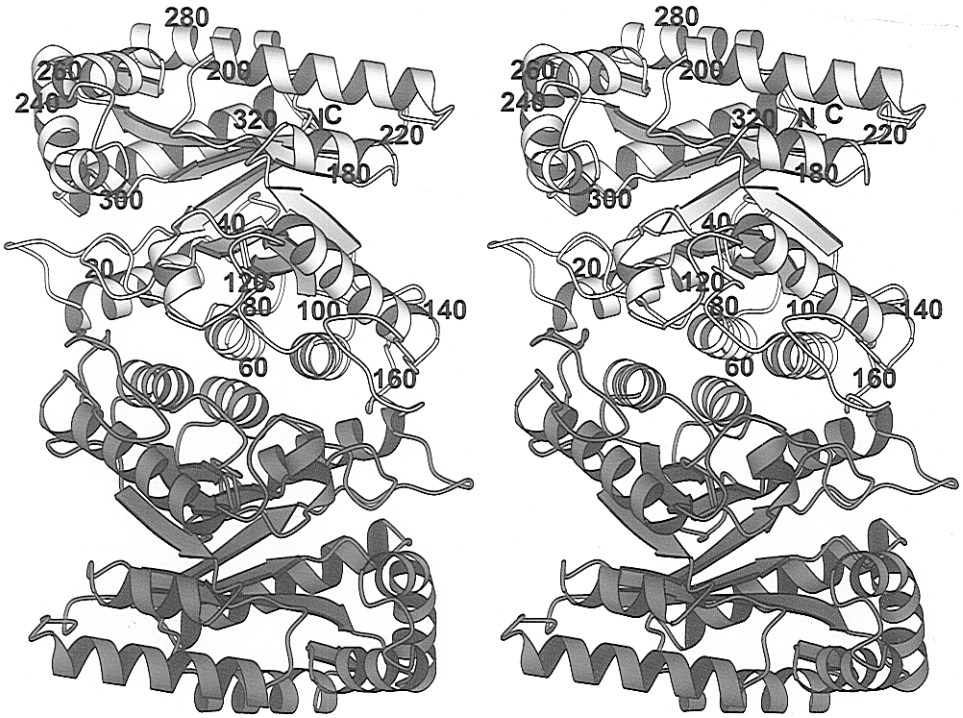

FIGURE 3: Ribbon drawing (stereo) of β_2 luciferase viewed down the dimer 2-fold axis. Subunits A and B are represented by light and dark ribbons, respectively. This orientation is similar to that used by Fisher et al. (1995) in their paper describing the $\alpha\beta$ structure. This figure and Figure 4 were made with Molscript (Kraulis, 1991).

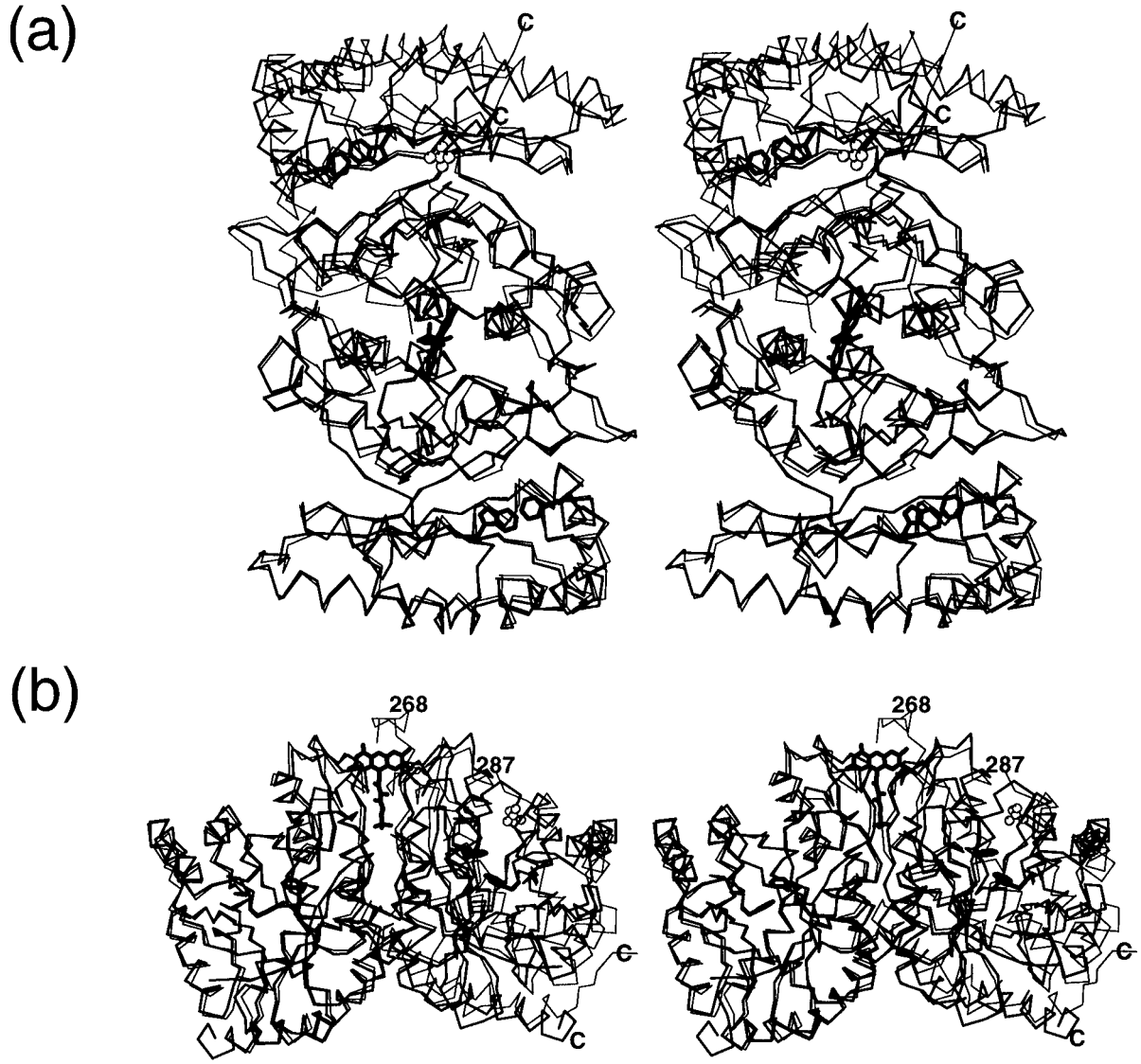

FIGURE 4: (a) C_α stereo drawing of β_2 luciferase (thick) viewed down the dimer 2-fold axis with the 2.4 Å $\alpha\beta$ luciferase structure (thin) superimposed. The β subunits are drawn in the lower half of the dimer. The upper half contains the A subunit of β_2 and the α subunit of $\alpha\beta$. FMN is modeled into the dimer interface active site we propose for the β_2 enzyme. The inorganic ion found in the α subunit of the $\alpha\beta$ structure is included for reference. Trp 194 and Phe 250 of β_2 are drawn to indicate the isoalloxazine binding pocket of the $\alpha\beta$ enzyme proposed by Fisher et al. (1995). (b) Same as in (a) except the 2-fold axis is vertical and the α subunit of the $\alpha\beta$ structure is on the right. Residues 268 and 287 of the α subunit of the $\alpha\beta$ structure, which are part of the mobile loop, are noted.

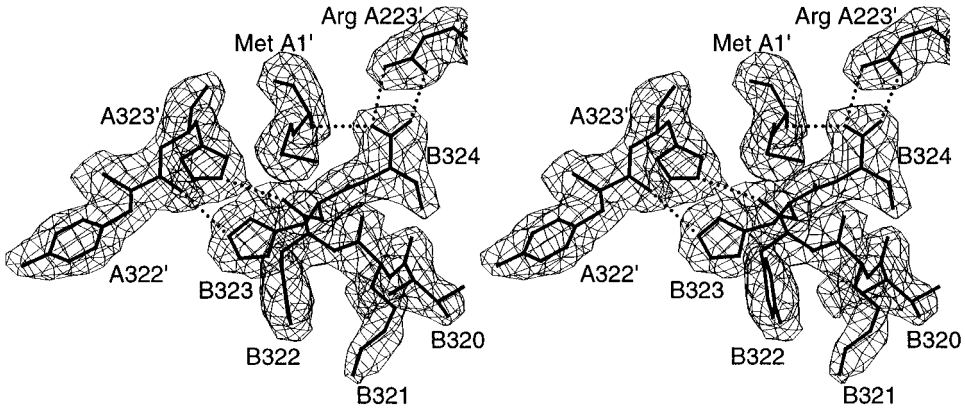

FIGURE 5: Stereo drawing of the C-terminal residues of subunit B of β_2 with $2F_o - F_c$ density contoured at 1σ. Note the axis of the 320's helix is vertical. Dots indicate salt links and hydrogen bonds to crystallographic neighbors. The primed residues are related by crystallographic symmetry to residues of subunit A.

the β_2 structure (Figure 4). Note that this is due to the fact that the conformations of the 170's loops of the α and β subunits differ. Second, the 256−289 mobile loop is unique to the α subunit. Although residues 272−289 are missing from the $\alpha\beta$ structure, enough of the loop is resolved to show that it passes through the molecular 2-fold axis and thereby

Table 1: Dimer Interfaces of β_2 and $\alpha\beta$ Luciferase[a]

	β_2	$\alpha\beta$[b]
A_s buried in interface (Å^2)	3794	4421
A_s buried by hydrophobic residues (Å^2)	2000	2183
A_s buried by charged residues (Å^2)	916	1117
intersubunit hydrogen bonds (3.6 Å cutoff)	5	10
intersubunit hydrogen bonds (4.0 Å cutoff)	10	18
intersubunit salt links (4.0 Å cutoff)	3	2
intersubunit salt links (5.0 Å cutoff)	3	5

[a] A_s calculated with X-PLOR using a probe radius of 1.4 Å. Hydrophobic includes Ala, Val, Ile, Leu, Met, Phe, Trp, and Pro. Charged includes Asp, Glu, Arg, Lys, and His. Hydrogen bonds calculated with X-PLOR using a 90° angle cutoff. No angle cutoff for salt links. [b] 2.4 Å $\alpha\beta$ structure (Fisher et al., 1995).

blocks an entrance to the dimer interface (Figure 4b). We will show evidence later that the active site of β_2 is in this part of the dimer interface.

Dimer Interface. The dimer interface buries 3794 Å^2 of solvent-accessible surface area (A_s) (Table 1). This value is in good agreement with empirical estimates based on molecular weight (Jones & Thorton, 1995). Most of the intersubunit interactions are hydrophobic, with 53% of the interface area contributed by hydrophobic residues and 24% from charged residues. Our calculations show that $\alpha\beta$ luciferase has a larger interface and buries 4421 Å^2 of A_s, or about 2210 Å^2 per subunit (Fisher et al., 1995). The contribution from hydrophobic and charged residues is 49% and 25%, respectively. The larger dimer interface in the $\alpha\beta$ structure is partly due to residues 256−271 of the α subunit, which are part of a loop that is absent from the β subunit. If residues 256−271 of the α subunit of $\alpha\beta$ luciferase are omitted, then the dimer interface area reduces to 4030 Å^2.

We calculated the number of intersubunit hydrogen bonds and salt links in the $\alpha\beta$ and β_2 structures to gauge the relative stabilities of the two interfaces (Table 1). The $\alpha\beta$ structure has more intersubunit hydrogen bonds and salt links; this result is independent of cutoff values. Since the $\alpha\beta$ dimer interface also buries more surface area, we conclude that its interface has more favorable energetics than the β_2 interface. This conclusion is in agreement with the idea that the heterodimer is more stable thermodynamically and that kinetic partitioning between folding pathways determines which dimer is formed (Sinclair et al., 1994).

We now discuss some of the intersubunit salt links and hydrogen bonds. Two of the three salt links in the β_2 interface are related by the molecular 2-fold axis and are

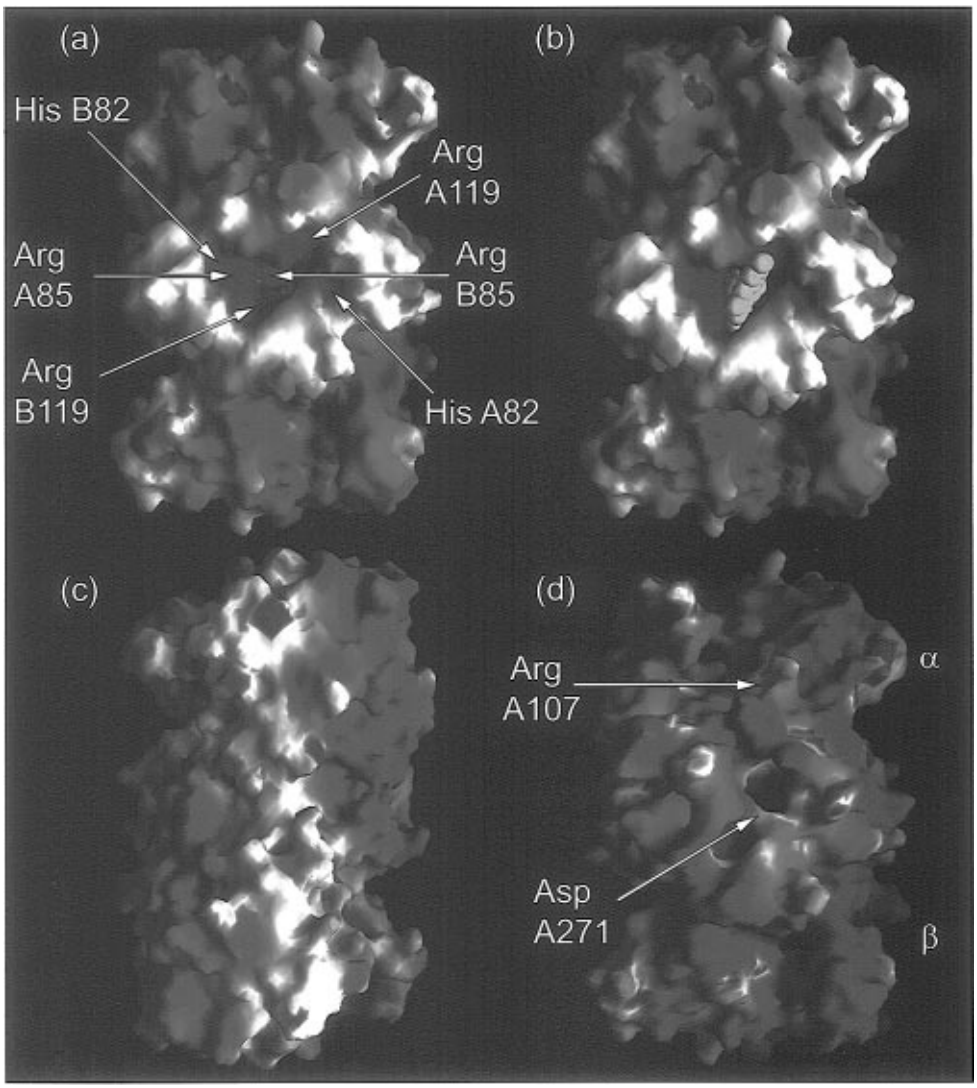

FIGURE 6: Electrostatic surfaces of β_2 (a−c) and $\alpha\beta$ (d) made with GRASP (Nicholls & Honig, 1992). Calculations assumed Asp, Glu, Arg, Lys, and His to be charged. (a) β_2 structure viewed down the 2-fold axis looking into the active site. (b) Same as (a) but with FMN modeled into the proposed active site. (c) Same as (a) but rotated 180° around the vertical axis. (d) 2.4 Å $\alpha\beta$ structure in same orientation as in (a).

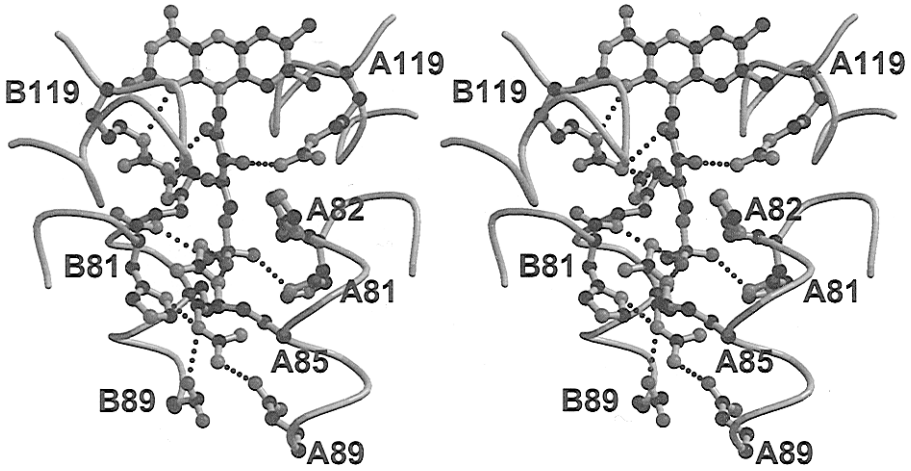

FIGURE 7: View of the proposed active site of the β_2 luciferase homodimer including a model of how the $FMNH_2$ substrate might bind. Dots indicate hydrogen bonds and salt links, and they represent distances <3.6 Å. Note that there are eight salt links and hydrogen bonds between the protein and FMN in this model. Carbon atoms are in black; all other atoms are in shades of gray. This figure was made with Molscript (Kraulis, 1991) and Raster3D (Merritt & Murphy, 1994).

formed between His 45 and Glu 88. These residues are conserved in the α subunit and the salt links are seen in the αβ structure. In addition, a water molecule that hydrogen bonds to the carboxylate of Glu 88 in β_2 is also seen in the 2.4 Å αβ structure. The intersubunit salt link between Arg B85 and Glu A89 is unique to the β_2 enzyme. Arg B85 of β_2 adopts a different conformation than is observed in the αβ structure. Arg B85 appears to change conformation to avoid the side chain of His A81, which is Ala in the αβ structure. The 2-fold related salt link (A85 Arg−B89 Glu) is not formed because the side chain conformations of Arg A85 and Arg B85 do not obey the approximate 2-fold symmetry. Rather, Arg A85 hydrogen bonds to Thr B80.

In addition to the Arg A85−Thr B80 hydrogen bond in the β_2 dimer interface, there is a hydrogen bond between Thr A57 and Glu B89 and also symmetric hydrogen bonds between Asn A159 and Ser B47 from both subunits. Finally, the side chains of Thr A57 and Thr B57 form a hydrogen bond (OG1−OG1 distance = 3.7 Å). This is a notable interaction because the midpoint of the hydrogen bond coincides with the location of the molecular 2-fold axis. This hydrogen bond is not made in αβ luciferase because residue 57 of the α subunit is Val.

Active Site. The αβ form of bacterial luciferase has been proposed to have a single $FMNH_2$ binding site located at the C-terminal end of the α subunit's β-barrel. The most compelling structural evidence is the location of an inorganic PO_4 or SO_4 ion in the 2.4 Å αβ crystal structure (see Figure 4) which is thought to represent the 5′-monophosphate of the substrate (Baldwin et al., 1995; Fisher et al., 1995). This ion forms a salt link to Arg 107, a conserved residue in all bacterial luciferase α subunits. Fisher et al. (1995) suggest that the isoalloxazine ring would contact Trp 194 and Trp 250 (Phe 250 in the β subunit), which is consistent with spectroscopic data. This location for the $FMNH_2$ binding site is also consistent with mutagenesis data involving His 44, Asp 113, and Cys 106.

However, there are several reasons why it is unlikely that $FMNH_2$ binds to β_2 in the same fashion. First, an inorganic ion (PO_4 or SO_4) was not found in the β subunit of the 2.4 Å αβ luciferase structure even though the crystallization solution contained 1.4 M SO_4 and 0.2 M PO_4. Second, the equivalent PO_4 site in the β_2 structure is occluded by Thr 175 due to rearrangement of the 170's loop (Figure 4a). Third, Arg 107 of the α subunit—the crucial residue that salt links to the ion in the αβ structure—is replaced by Asp in the β subunit. The nearest basic residue in our structure that could take the place of Arg 107 is Arg 193, whose guanidinium group is 5−7 Å from the proposed PO_4 site but is occupied in salt links with Asp 196 and Asp 195. Finally, if $FMNH_2$ binds to β_2 in the site proposed for αβ luciferase, then there would be two binding sites per homodimer, which would contradict biochemical data (Choi et al., 1995).

We propose that the $FMNH_2$ binding site of β_2 is different from that proposed for αβ. Inspection of the β_2 structure reveals a plausible FMN binding site in the dimer interface in which the ribityl chain is nearly coincident with the molecular 2-fold axis as shown in Figure 4b. This site is appropriate because it has an unusually high density of basic residues that are poised to bind the ribityl and 5′-monophosphate of FMN, it is solvent accessible, and it has the right size and shape to accommodate FMN.

The electrostatic surface of β_2 with a view looking into the proposed $FMNH_2$ binding site is shown in Figure 6a. The binding site is a crevice bathed in positive electrostatic field (Figure 6a), and it readily accommodates an FMN molecule (Figure 6b).

The details of the proposed flavin binding site are shown in Figure 7. FMN was modeled manually into the site without making adjustments to the protein residues. Next, the FMN was allowed to relax using conjugate gradient minimization in X-PLOR while fixing the protein atoms. The closest FMN−protein contact is 2.5 Å and is between Arg B119 CD and FMN O2 of the isoalloxazine ring. This contact would be relieved easily if the protein was allowed to relax in response to the FMN. The geometry of the FMN is not distorted.

There are three salt links to the 5′-monophosphate involving His A81 and Arg A85 and one hydrogen bond to the PO_4 with the main chain of His B82 (Figure 7). Arg A119 and Arg B119 hydrogen bond to the ribityl chain, and in addition Arg B119 hydrogen bonds to N1 of the isoalloxazine ring. The guanidinium of Arg B85 sits at the bottom of the binding site and is stabilized by salt links to Glu A89 and Glu B89 and by a hydrogen bond to His B81 (electron

density connects its ND1 atom and Arg B85 NE).

Although the active sites of enzymes with the $(\beta/\alpha)_8$ motif typically are found at the C-terminal end of the β-barrel, for example glycolate oxidase (Lindqvist, 1989), there is precedence for binding flavin in a dimer interface. Flavin reductase P from *V. harveyi* (Tanner et al., 1996), NADH oxidase from *Thermus thermophilus* (Hecht et al., 1995), and the *lux*F protein from *Photobacterium leiognathi* (Moore et al., 1993) bind flavin cofactors in the dimer interface. The latter protein contains a β-barrel motif.

In our model the flavin is recognized mainly by its 5′-monophosphate and ribityl chain. The isoalloxazine ring has high solvent exposure (Figure 6b) compared with flavins bound to other flavoproteins, for example flavin reductase P (Tanner et al., 1996). Solvent exposure would adversely affect the yields and/or reactivities of 4a-oxygenated flavin intermediates or substantially reduce the emission efficiency of the excited emitter when formed (Ghisla et al., 1974; Kemal & Bruice, 1976). Therefore, our model offers an explanation of why β_2 is less active than $\alpha\beta$ (Sinclair et al., 1993; Waddle & Baldwin, 1991).

The proposed site has good shape complementarity to an FMN, and recognition of the 5′-monophosphate is an important aspect of binding. We therefore predict that reduced FAD and riboflavin would be less suitable substrates for β_2. FAD would be rejected on the basis of steric overlap involving the adenine half of the molecule. Riboflavin would fit in the binding pocket but could not take full advantage of the cluster of basic residues in the active site.

Recent kinetics and gel filtration experiments suggest that there is only one $FMNH_2$ binding site per β_2 homodimer (Choi et al., 1995). Inspection of the surface of β_2 confirms this hypothesis. A second view of the β_2 electrostatic surface is in Figure 6c. It shows that there is not a second binding site along the 2-fold axis on the "back side" of the dimer.

Finally, would the proposed flavin site be functional in the $\alpha\beta$ heterodimer? Sequence identity between the α and β subunits suggests that the binding site is partially formed in the $\alpha\beta$ heterodimer. In our proposed binding site, Arg 85 and His 82 are conserved in the *V. harveyi* α and β subunits, while residues 81 and 119 are not conserved. They are Ala and Thr, respectively, in the α subunit rather than His and Arg as in the β subunit. Indeed, the $\alpha\beta$ structure also presents a large positive electrostatic field in the binding site that we propose (Figure 6d). However, access to the binding site is blocked by the mobile loop (residues 257−289) that is unique to the α subunit, particularly by Asp 271 (Figure 6d).

These observations raise two intriguing scenarios. First, perhaps the mobile loop of the α subunit plays a functional role by preventing the dimer interface flavin binding site from competing with the flavin binding site in the α subunit. A second possibility is that the dimer interface binding site that we have identified is the *true* flavin binding site of both the β_2 and the $\alpha\beta$ enzymes. The mobile loop in this case could act like a gate to the active site in the dimer interface and would protect it from solvent when the gate is closed. The electrostatic surfaces of the β_2 and $\alpha\beta$ structures support this idea because in both cases our proposed site presents a strong positive electrostatic field, whereas the site proposed by others (Baldwin et al., 1995; Fisher et al., 1995) displays a negative field (Figure 6). If we are correct, then the reason for the low activity of β_2 may be that it lacks the gate. The answers to these questions will have to await definitive structural determination of the location of the active site.

REFERENCES

Baldwin, T. O., & Ziegler, M. M. (1992) in *Chemistry and Biochemistry of Flavoenzymes* (Müller, F., Ed.) pp 467−530, CRC Press, Boca Raton, FL.

Baldwin, T. O., Christopher, J. A., Raushel, F. M., Sinclair, J. F., Ziegler, M. M., Fisher, A. J., & Rayment, I. (1995) *Curr. Opin. Struct. Biol. 5*, 798−809.

Baldwin, T., Raushel, F., Rayment, I., Fisher, A., & Thoden, J. (1997) in *Flavins and Flavoproteins* (Stevenson, K. J., Massey, V., & Williams, C. H., Jr., Eds.) University of Calgary Press, Calgary, Alberta, Canada.

Brünger, A. T. (1992) *X-PLOR version 3.1, A system for X-ray crystallography and NMR*, Yale University Press, New Haven, CT.

Choi, H., Tang, C.-K., & Tu, S.-C. (1995) *J. Biol. Chem. 270*, 16813−16819.

Cousineau, J., & Meighen, E. A. (1976) *Biochemistry 15*, 4992−5000.

Engh, R. A., & Huber, R. (1991) *Acta Crystallogr. A47*, 392−400.

Fisher, A. J., Raushel, F. M., Baldwin, T. O., & Rayment, I. (1995) *Biochemistry 34*, 6581−6586.

Fisher, A. J., Thompson, T. B., Thoden, J. B., Baldwin, T. O., & Rayment, I. (1996) *J. Biol. Chem. 271*, 21956−21968.

Friedland, J., & Hastings, J. W. (1967) *Proc. Natl. Acad. Sci. U.S.A. 58*, 2336−2342.

Ghisla, S., Massey, V., Lhoste, J.-M., & Mayhew, S. G. (1974) *Biochemistry 13*, 589−597.

Gunsalus-Miguel, A., Meighen, E. A., Nicoli, M. Z., Nealson, K. H., & Hastings, J. W. (1972) *J. Biol. Chem. 247*, 398−404.

Hastings, J. W., Weber, K., Friedland, J., Eberhard, A., Mitchell, G. W., & Gunsalus, A. (1969) *Biochemistry 8*, 4681−4689.

Hecht, H. J., Erdmann, H., Park, H. J., Sprinzl, M., & Schmid, R. D. (1995) *Nat. Struct. Biol. 2*, 1109−1114.

Jones, S., & Thorton, J. M. (1995) *Prog. Biophys. Mol. Biol. 63*, 31−65.

Jones, T. A., Zou, J.-Y., Cowan, S. W., & Kjeldgaard, M. (1991) *Acta Crystallogr. A47*, 110−119.

Kemal, C., & Bruice, T. C. (1976) *Proc. Natl. Acad. Sci. U.S.A. 73*, 995−999.

Kleywegt, G. J., & Brünger, A. T. (1996) *Structure 4*, 897−904.

Kraulis, P. J. (1991) *J. Appl. Crystallogr. 24*, 946−950.

Laskowski, R. A., MacArthur, M. W., Moss, D. S., & Thornton, J. M. (1993) *J. Appl. Crystallogr. 26*, 283−291.

Lindqvist, Y. (1989) *J. Mol. Biol. 209*, 151−166.

Luzzati, P. V. (1952) *Acta Crystallogr. 5*, 802−810.

Merritt, E. A., & Murphy, M. E. P. (1994) *Acta Crystallogr. D50*, 869−873.

Minor, W. (1993) XDISPLAYF Program, Purdue University.

Moore, S. A., James, M. N. G., O'Kane, D. J., & Lee, J. (1993) *EMBO J. 12*, 1767−1774.

Nicholls, A., & Honig, B. (1992) Columbia University, New York.

Otwinowski, Z. (1993) in *CCP4 Study Weekend: Data Collection and Processing* (Sawyer, L., Isaacs, N., & Bailey, S., Eds.) pp 56−62, SERC Daresbury Laboratory, Warrington, England.

Read, R. J. (1986) *Acta Crystallogr. A42*, 140−149.

Ruby, E. G., & Hastings, J. W. (1980) *Biochemistry 19*, 4989−4993.

Sinclair, J. F., Waddle, J. J., Waddill, E. F., & Baldwin, T. O. (1993) *Biochemistry 32*, 5036−5044.

Sinclair, J. F., Ziegler, M. M., & Baldwin, T. O. (1994) *Nat. Struct. Biol. 1*, 320−326.

Tanner, J. J., Lei, B., Tu, S.-C., & Krause, K. L. (1996) *Biochemistry 35*, 13531−13539.

Tu, S.-C., & Mager, H. I. X. (1995) *Photochem. Photobiol. 62*, 615−624.

Waddle, J., & Baldwin, T. O. (1991) *Biochem. Biophys. Res. Commun. 178*, 1188−1193.

Xi, L., Cho, K. W., Herndon, M. E., & Tu, S.-C. (1990) *J. Biol. Chem. 265*, 4200−4203.

BI962511X